

New Strategies to Obtain Insights into CP Violation Through $B_s \rightarrow D_s^\pm K^\mp, D_s^{*\pm} K^\mp, \dots$ and $B_d \rightarrow D^\pm \pi^\mp, D^{*\pm} \pi^\mp, \dots$ Decays

Robert Fleischer

Theory Division, CERN, CH-1211 Geneva 23, Switzerland

Abstract

Decays of the kind $B_s \rightarrow D_s^\pm K^\mp, D_s^{*\pm} K^\mp, \dots$ and $B_d \rightarrow D^\pm \pi^\mp, D^{*\pm} \pi^\mp, \dots$ allow us to probe $\phi_s + \gamma$ and $\phi_d + \gamma$, respectively, involving the angle γ of the unitarity triangle and the $B_q^0 - \bar{B}_q^0$ mixing phases ϕ_q ($q \in \{d, s\}$). Analysing these modes in a phase-convention-independent way, we find that their mixing-induced observables are affected by a subtle $(-1)^L$ factor, where L denotes the angular momentum of the B_q decay products, and derive bounds on $\phi_q + \gamma$. Moreover, we emphasize that “untagged” rates are an important ingredient for efficient determinations of weak phases, not only in the presence of a sizeable width difference $\Delta\Gamma_q$; should $\Delta\Gamma_s$ be sizeable, the combination of “untagged” with “tagged” $B_s \rightarrow D_s^\pm K^\mp, D_s^{*\pm} K^\mp, \dots$ observables provides an elegant and *unambiguous* extraction of $\tan(\phi_s + \gamma)$, whereas the “conventional” determination of $\phi_s + \gamma$ is affected by an eightfold discrete ambiguity. Finally, we propose a *combined* analysis of $B_s \rightarrow D_s^\pm K^\mp, D_s^{*\pm} K^\mp, \dots$ and $B_d \rightarrow D^\pm \pi^\mp, D^{*\pm} \pi^\mp, \dots$ modes, which has important advantages, offering various interesting new strategies to extract γ in an essentially unambiguous manner.

1 Introduction

The exploration of CP violation through studies of B -meson decays is one of the most exciting topics of present particle physics phenomenology, the main goal being to perform stringent tests of the Kobayashi–Maskawa mechanism [1]. Here the central target is the unitarity triangle of the Cabibbo–Kobayashi–Maskawa (CKM) matrix, with its angles α , β and γ (for a detailed review, see [2]). Thanks to the efforts of the BaBar (SLAC) and Belle (KEK) collaborations, CP violation could recently be established in the neutral B_d -meson system with the help of $B_d \rightarrow J/\psi K_S$ and similar decays [3]. These modes allow us to determine $\sin \phi_d$, where the present world average is given by $\sin \phi_d = 0.734 \pm 0.054$ [4], implying the twofold solution $\phi_d = (47^{+5}_{-4})^\circ \vee (133^{+4}_{-5})^\circ$ for the $B_d^0\text{--}\overline{B}_d^0$ mixing phase ϕ_d , which equals 2β in the Standard Model. Here the former solution would be in perfect agreement with the “indirect” range following from the Standard-Model “CKM fits”, $40^\circ \lesssim \phi_d \lesssim 60^\circ$ [5], whereas the latter would correspond to new physics [6]. Measuring the sign of $\cos \phi_d$, the two solutions can be distinguished. Several strategies to accomplish this important task were proposed [7]; an analysis using the time-dependent angular distribution of the decay products of $B_d \rightarrow J/\psi[\rightarrow \ell^+ \ell^-] K^*[\rightarrow \pi^0 K_S]$ [8, 9] is already in progress at the B factories [10].

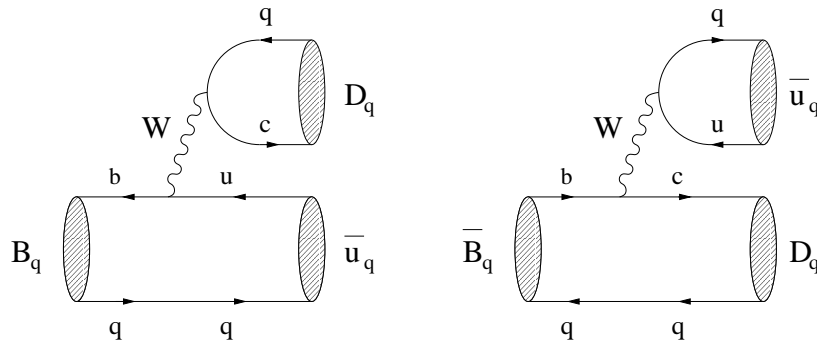


Figure 1: Feynman diagrams contributing to $B_q^0 \rightarrow D_q \overline{u}_q$ and $\overline{B}_q^0 \rightarrow D_q \overline{u}_q$.

An important ingredient for the testing of the Kobayashi–Maskawa picture is provided by transitions of the kind $B_s \rightarrow D_s^\pm K^\mp, D_s^{*\pm} K^\mp, \dots$ [11] and $B_d \rightarrow D^\pm \pi^\mp, D^{*\pm} \pi^\mp, \dots$ [12], allowing theoretically clean determinations of the weak phases $\phi_s + \gamma$ and $\phi_d + \gamma$, respectively, where ϕ_s is the B_s -meson counterpart of ϕ_d , which is negligibly small in the Standard Model. It is convenient to write these decays generically as $B_q^0 \rightarrow D_q \overline{u}_q$, so that we may easily distinguish between the following cases:

- $q = s$: $D_s \in \{D_s^+, D_s^{*+}, \dots\}$, $u_s \in \{K^+, K^{*+}, \dots\}$,
- $q = d$: $D_d \in \{D^+, D^{*+}, \dots\}$, $u_d \in \{\pi^+, \rho^+, \dots\}$.

In the discussion given below, we shall only consider $B_q^0 \rightarrow D_q \overline{u}_q$ decays, where at least one of the D_q, \overline{u}_q states is a pseudoscalar meson. In the opposite case, for example the $B_s^0 \rightarrow D_s^{*+} K^{*-}$ decay, the extraction of weak phases would require a complicated angular

analysis [13]–[15]. If we look at Fig. 1, we observe that $B_q^0 \rightarrow D_q \bar{u}_q$ originates from colour-allowed tree-diagram-like topologies, and that also a \bar{B}_q^0 meson may decay into the same final state $D_q \bar{u}_q$. The latter feature leads to interference effects between B_q^0 – \bar{B}_q^0 mixing and decay processes, allowing the extraction of $\phi_q + \gamma$ with an eightfold discrete ambiguity. Since ϕ_q can be straightforwardly fixed separately [2], we may determine the angle γ of the unitarity triangle from this CP-violating weak phase.

In Section 2, we focus on the $B_q \rightarrow D_q \bar{u}_q$ decay amplitudes and rate asymmetries, and investigate the relevant hadronic parameters with the help of “factorization”. In this section, we shall also point out that a subtle factor $(-1)^L$ arises in the expressions for the mixing-induced observables, where L denotes the angular momentum of the $D_q \bar{u}_q$ system, and show explicitly the cancellation of phase-convention-dependent parameters within the factorization approach. After discussing the “conventional” extraction of $\phi_q + \gamma$ and the associated multiple discrete ambiguities in Section 3, we emphasize the usefulness of “untagged” rate measurements for efficient determinations of weak phases from $B_q \rightarrow D_q \bar{u}_q$ decays in Section 4, and suggest several novel strategies. In Section 5, we then derive bounds on $\phi_q + \gamma$, and illustrate their potential power with the help of a few numerical examples. In Section 6, we propose a *combined* analysis of $B_s \rightarrow D_s \bar{u}_s$ and $B_d \rightarrow D_d \bar{u}_d$ modes, which has important advantages with respect to the conventional separate determinations of $\phi_s + \gamma$ and $\phi_d + \gamma$, offering various attractive new avenues to extract γ in an essentially unambiguous manner and to obtain valuable insights into hadron dynamics. Finally, we conclude in Section 7.

2 Amplitudes, Rate Asymmetries and Factorization

2.1 Amplitudes

The $B_q \rightarrow D_q \bar{u}_q$ decays are the colour-allowed counterparts of the $B_s \rightarrow D \eta^{(\prime)}, D \phi, \dots$ and $B_d \rightarrow D \pi^0, D \rho^0, \dots$ channels, which were recently analysed in detail in [16, 17]. If we follow the same avenue, and take also the Feynman diagrams shown in Fig. 1 into account, we may write

$$A(\bar{B}_q^0 \rightarrow D_q \bar{u}_q) = \langle \bar{u}_q D_q | \mathcal{H}_{\text{eff}}(\bar{B}_q^0 \rightarrow D_q \bar{u}_q) | \bar{B}_q^0 \rangle = \frac{G_F}{\sqrt{2}} \bar{v}_q \bar{M}_q, \quad (2.1)$$

where the hadronic matrix element

$$\bar{M}_q \equiv \langle \bar{u}_q D_q | \bar{\mathcal{O}}_1^q C_1(\mu) + \bar{\mathcal{O}}_2^q C_2(\mu) | \bar{B}_q^0 \rangle \quad (2.2)$$

involves the current–current operators

$$\bar{\mathcal{O}}_1^q \equiv (\bar{q}_\alpha u_\beta)_{V-A} (\bar{c}_\beta b_\alpha)_{V-A}, \quad \bar{\mathcal{O}}_2^q \equiv (\bar{q}_\alpha u_\alpha)_{V-A} (\bar{c}_\beta b_\beta)_{V-A}. \quad (2.3)$$

The CKM factors \bar{v}_q are given by

$$\bar{v}_s \equiv V_{us}^* V_{cb} = A \lambda^3, \quad \bar{v}_d \equiv V_{ud}^* V_{cb} = A \lambda^2 (1 - \lambda^2/2), \quad (2.4)$$

with (for the numerical value, see [18])

$$A \equiv \frac{1}{\lambda^2} |V_{cb}| = 0.83 \pm 0.02, \quad (2.5)$$

and $\lambda \equiv |V_{us}| = 0.22$ is the usual Wolfenstein parameter [19].

On the other hand, the $B_q^0 \rightarrow D_q \bar{u}_q$ decay amplitude takes the following form:

$$\begin{aligned} A(B_q^0 \rightarrow D_q \bar{u}_q) &= \langle \bar{u}_q D_q | \mathcal{H}_{\text{eff}}(B_q^0 \rightarrow D_q \bar{u}_q) | B_q^0 \rangle \\ &= \frac{G_F}{\sqrt{2}} v_q^* \langle \bar{u}_q D_q | \mathcal{O}_1^{q\dagger} C_1(\mu) + \mathcal{O}_2^{q\dagger} C_2(\mu) | B_q^0 \rangle, \end{aligned} \quad (2.6)$$

where we have to deal with the current-current operators

$$\mathcal{O}_1^q \equiv (\bar{q}_\alpha c_\beta)_{V-A} (\bar{u}_\beta b_\alpha)_{V-A}, \quad \mathcal{O}_2^q \equiv (\bar{q}_\alpha c_\alpha)_{V-A} (\bar{u}_\beta b_\beta)_{V-A}, \quad (2.7)$$

and the CKM factors v_q are given by

$$v_s \equiv V_{cs}^* V_{ub} = A \lambda^3 R_b e^{-i\gamma}, \quad v_d \equiv V_{cd}^* V_{ub} = - \left(\frac{A \lambda^4 R_b}{1 - \lambda^2/2} \right) e^{-i\gamma}, \quad (2.8)$$

with (for the numerical value, see [18])

$$R_b \equiv \left(1 - \frac{\lambda^2}{2} \right) \frac{1}{\lambda} \left| \frac{V_{ub}}{V_{cb}} \right| = \sqrt{\bar{\rho}^2 + \bar{\eta}^2} = 0.39 \pm 0.04. \quad (2.9)$$

If we introduce convention-dependent CP phases through

$$(\mathcal{CP})|F\rangle = e^{i\phi_{\text{CP}}(F)} |\bar{F}\rangle, \quad (\mathcal{CP})|\bar{F}\rangle = e^{-i\phi_{\text{CP}}(F)} |F\rangle \quad (2.10)$$

for $F \in \{B_q, D_q, u_q\}$, we obtain

$$(\mathcal{CP})|D_q \bar{u}_q\rangle = (-1)^L e^{i[\phi_{\text{CP}}(D_q) - \phi_{\text{CP}}(u_q)]} |\bar{D}_q u_q\rangle, \quad (2.11)$$

where L denotes the angular momentum of the $D_q \bar{u}_q$ state. As we shall see below, the subtle $(-1)^L$ factor enters in mixing-induced observables, and plays an important rôle for the extraction of weak phases from these quantities in the presence of non-trivial angular momenta, for instance in the case of $B_d^0 \rightarrow D^{*+} \pi^-$. In the literature, this factor does not show up explicitly in the context of $B_q^0 \rightarrow D_q \bar{u}_q$ modes, but it was recently pointed out in the analysis of their colour-suppressed counterparts in [16, 17]. If we now employ, as in these papers, the operator relations

$$(\mathcal{CP})^\dagger (\mathcal{CP}) = \hat{1}, \quad (2.12)$$

$$(\mathcal{CP}) \mathcal{O}_k^{q\dagger} (\mathcal{CP})^\dagger = \mathcal{O}_k^q, \quad (2.13)$$

we may rewrite (2.6) as

$$A(B_q^0 \rightarrow D_q \bar{u}_q) = (-1)^L e^{i[\phi_{\text{CP}}(B_q) - \phi_{\text{CP}}(D_q) + \phi_{\text{CP}}(u_q)]} \frac{G_F}{\sqrt{2}} v_q^* M_q, \quad (2.14)$$

where

$$M_q \equiv \langle u_q \bar{D}_q | \mathcal{O}_1^q C_1(\mu) + \mathcal{O}_2^q C_2(\mu) | \bar{B}_q^0 \rangle. \quad (2.15)$$

It should be noted that also certain exchange topologies contribute to $B_q^0 \rightarrow D_q \bar{u}_q$, $\bar{B}_q^0 \rightarrow D_q \bar{u}_q$ transitions, which were – for simplicity – not shown in Fig. 1. However, these additional diagrams do not affect the phase structure of the amplitudes in (2.1) and (2.14), and manifest themselves only through tiny contributions to the hadronic matrix elements \bar{M}_q and M_q given in (2.2) and (2.15), respectively. We shall come back to these topologies in Subsection 4.2, noting also how they may be probed experimentally.

An analogous calculation for the $\bar{B}_q^0 \rightarrow \bar{D}_q u_q$ and $B_q^0 \rightarrow \bar{D}_q u_q$ processes yields

$$A(\bar{B}_q^0 \rightarrow \bar{D}_q u_q) = \frac{G_F}{\sqrt{2}} v_q M_q \quad (2.16)$$

$$A(B_q^0 \rightarrow \bar{D}_q u_q) = (-1)^L e^{i[\phi_{\text{CP}}(B_q) + \phi_{\text{CP}}(D_q) - \phi_{\text{CP}}(u_q)]} \frac{G_F}{\sqrt{2}} \bar{v}_q^* \bar{M}_q, \quad (2.17)$$

where the same hadronic matrix elements as in the $B_q^0 \rightarrow D_q \bar{u}_q$, $\bar{B}_q^0 \rightarrow D_q \bar{u}_q$ modes arise.

2.2 Rate Asymmetries

Let us first consider B_q decays into $D_q \bar{u}_q$. Since both a B_q^0 and a \bar{B}_q^0 meson may decay into this state, we obtain a time-dependent rate asymmetry of the following form [2]:

$$\begin{aligned} & \frac{\Gamma(B_q^0(t) \rightarrow D_q \bar{u}_q) - \Gamma(\bar{B}_q^0(t) \rightarrow D_q \bar{u}_q)}{\Gamma(B_q^0(t) \rightarrow D_q \bar{u}_q) + \Gamma(\bar{B}_q^0(t) \rightarrow D_q \bar{u}_q)} \\ &= \left[\frac{C(B_q \rightarrow D_q \bar{u}_q) \cos(\Delta M_q t) + S(B_q \rightarrow D_q \bar{u}_q) \sin(\Delta M_q t)}{\cosh(\Delta \Gamma_q t/2) - \mathcal{A}_{\Delta\Gamma}(B_q \rightarrow D_q \bar{u}_q) \sinh(\Delta \Gamma_q t/2)} \right], \end{aligned} \quad (2.18)$$

where $\Delta M_q \equiv M_{\text{H}}^{(q)} - M_{\text{L}}^{(q)} > 0$ is the mass difference of the B_q mass eigenstates B_q^{H} (“heavy”) and B_q^{L} (“light”), and $\Delta \Gamma_q \equiv \Gamma_{\text{H}}^{(q)} - \Gamma_{\text{L}}^{(q)}$ denotes their decay width difference, providing the observable $\mathcal{A}_{\Delta\Gamma}(B_q \rightarrow D_q \bar{u}_q)$. Before we turn to this quantity in the context of the “untagged” rates discussed in Subsection 4.1, let us first focus on $C(B_q \rightarrow D_q \bar{u}_q)$ and $S(B_q \rightarrow D_q \bar{u}_q)$. These observables are given by

$$C(B_q \rightarrow D_q \bar{u}_q) \equiv C_q = \frac{1 - |\xi_q|^2}{1 + |\xi_q|^2}, \quad S(B_q \rightarrow D_q \bar{u}_q) \equiv S_q = \frac{2 \text{Im} \xi_q}{1 + |\xi_q|^2}, \quad (2.19)$$

where

$$\xi_q \equiv -e^{-i\phi_q} \left[\frac{A(\bar{B}_q^0 \rightarrow D_q \bar{u}_q)}{A(B_q^0 \rightarrow D_q \bar{u}_q)} \right] \quad (2.20)$$

measures the strength of the interference effects between the $B_q^0\text{--}\overline{B}_q^0$ mixing and decay processes, involving the CP-violating weak $B_q^0\text{--}\overline{B}_q^0$ mixing phase

$$\phi_q \equiv 2 \arg(V_{tq}^* V_{tb}) \stackrel{\text{SM}}{=} \begin{cases} +2\beta = \mathcal{O}(50^\circ) & (q = d) \\ -2\lambda^2\eta = \mathcal{O}(-2^\circ) & (q = s). \end{cases} \quad (2.21)$$

If we now insert (2.1) and (2.14) into (2.20), we observe that the convention-dependent phase $\phi_{\text{CP}}(B_q)$ is cancelled through the amplitude ratio, and arrive at

$$\xi_q = -(-1)^L e^{-i(\phi_q + \gamma)} \left[\frac{1}{x_q e^{i\delta_q}} \right], \quad (2.22)$$

where

$$x_s \equiv R_b a_s, \quad x_d \equiv - \left(\frac{\lambda^2 R_b}{1 - \lambda^2} \right) a_d, \quad (2.23)$$

with

$$a_q e^{i\delta_q} \equiv e^{-i[\phi_{\text{CP}}(D_q) - \phi_{\text{CP}}(u_q)]} \frac{M_q}{\overline{M}_q}. \quad (2.24)$$

The convention-dependent phases $\phi_{\text{CP}}(D_q)$ and $\phi_{\text{CP}}(u_q)$ in (2.24) are cancelled through the ratio of hadronic matrix elements, so that $a_q e^{i\delta_q}$ is actually a physical observable. Employing the factorization approach to deal with the hadronic matrix elements, we shall demonstrate this explicitly in Subsection 2.3. We may now apply (2.19), yielding

$$C_q = - \left[\frac{1 - x_q^2}{1 + x_q^2} \right], \quad S_q = (-1)^L \left[\frac{2 x_q \sin(\phi_q + \gamma + \delta_q)}{1 + x_q^2} \right]. \quad (2.25)$$

If we perform an analogous calculation for the decays into the CP-conjugate final state $\overline{D}_q u_q$, we obtain

$$\overline{\xi}_q = -e^{-i\phi_q} \left[e^{i\phi_{\text{CP}}(B_q)} \frac{A(\overline{B}_q^0 \rightarrow \overline{D}_q u_q)}{A(B_q^0 \rightarrow \overline{D}_q u_q)} \right] = -(-1)^L e^{-i(\phi_q + \gamma)} [x_q e^{i\delta_q}], \quad (2.26)$$

which implies

$$\overline{C}_q = + \left[\frac{1 - x_q^2}{1 + x_q^2} \right], \quad \overline{S}_q = (-1)^L \left[\frac{2 x_q \sin(\phi_q + \gamma - \delta_q)}{1 + x_q^2} \right], \quad (2.27)$$

where $\overline{C}_q \equiv C(B_q \rightarrow \overline{D}_q u_q)$ and $\overline{S}_q \equiv S(B_q \rightarrow \overline{D}_q u_q)$.

It should be noted that $\overline{\xi}_q$ and ξ_q satisfy the relation

$$\overline{\xi}_q \times \xi_q = e^{-i2(\phi_q + \gamma)}, \quad (2.28)$$

where the hadronic parameter $x_q e^{i\delta_q}$ cancels. Consequently, we may extract $\phi_q + \gamma$ in a *theoretically clean* way from the corresponding observables. For our purposes, it will be convenient to introduce the following quantities:

$$\langle C_q \rangle_+ \equiv \frac{\overline{C}_q + C_q}{2} = 0 \quad (2.29)$$

$$\langle C_q \rangle_- \equiv \frac{\overline{C}_q - C_q}{2} = \frac{1 - x_q^2}{1 + x_q^2} \quad (2.30)$$

$$\langle S_q \rangle_+ \equiv \frac{\overline{S}_q + S_q}{2} = +(-1)^L \left[\frac{2x_q \cos \delta_q}{1 + x_q^2} \right] \sin(\phi_q + \gamma) \quad (2.31)$$

$$\langle S_q \rangle_- \equiv \frac{\overline{S}_q - S_q}{2} = -(-1)^L \left[\frac{2x_q \sin \delta_q}{1 + x_q^2} \right] \cos(\phi_q + \gamma). \quad (2.32)$$

We observe that the factor $(-1)^L$ is crucial for the correctness of the sign of the mixing-induced observable combinations $\langle S_q \rangle_+$ and $\langle S_q \rangle_-$. In particular, if we fix the sign of $\cos \delta_q$ through factorization arguments, we may determine the sign of $\sin(\phi_q + \gamma)$ from the measured sign of $\langle S_q \rangle_+$, providing valuable information. If we consider, for example, $B_s \rightarrow D_s^{*\pm} K^\mp$ or $B_d \rightarrow D^{*\pm} \pi^\mp$ modes, we have $L = 1$, and obtain a non-trivial factor of $(-1)^1 = -1$. On the other hand, we have $(-1)^0 = +1$ in the case of $B_s \rightarrow D_s^\pm K^\mp$ or $B_d \rightarrow D^\pm \pi^\mp$ channels. Let us next analyse the hadronic parameter $a_q e^{i\delta_q}$ with the help of the factorization approach.

2.3 Factorization

Because of “colour-transparency” arguments [20, 21], the factorization of the hadronic matrix elements of four-quark operators into the product of hadronic matrix elements of two quark currents can be nicely motivated for the decay $\overline{B}_q^0 \rightarrow D_q \overline{u}_q$, involving the matrix element \overline{M}_q . Recently, this picture could be put on a much more solid theoretical basis [22]. On the other hand, these arguments do not apply to the $\overline{B}_q^0 \rightarrow \overline{D}_q u_q$ channel entering M_q , since there the spectator quark q ends up in the u_q meson, which is not “heavy” (see Fig. 1). In order to analyse the hadronic parameter $a_q e^{i\delta_q}$ introduced in (2.24), it is nevertheless instructive to apply “naïve” factorization not only to (2.2), but also to (2.15), yielding

$$\overline{M}_q|_{\text{fact}} = a_1 \langle \overline{u}_q | (\overline{q}_\alpha u_\alpha)_{V-A} | 0 \rangle \langle D_q | (\overline{c}_\beta b_\beta)_{V-A} | \overline{B}_q^0 \rangle \quad (2.33)$$

$$M_q|_{\text{fact}} = a_1 \langle \overline{D}_q | (\overline{q}_\alpha c_\alpha)_{V-A} | 0 \rangle \langle u_q | (\overline{u}_\beta b_\beta)_{V-A} | \overline{B}_q^0 \rangle, \quad (2.34)$$

where

$$a_1 = \frac{C_1(\mu_F)}{N_C} + C_2(\mu_F) \approx 1 \quad (2.35)$$

is the well-known phenomenological colour factor for colour-allowed decays [21], with a factorization scale μ_F and a number N_C of quark colours.

To be specific, let us consider the decays $\overline{B}_s^0 \rightarrow D_s^{(*)+} K^-$ and $\overline{B}_d^0 \rightarrow D^{(*)+} \pi^-$, i.e. $u_s = K^+$, $u_d = \pi^+$ and $D_s = D_s^{(*)+}$, $D_d = D^{(*)+}$. Using (2.10) and (2.12), as well as

$$(\mathcal{CP}) [\overline{q} \gamma^\mu (1 - \gamma_5) u] (\mathcal{CP})^\dagger = - [\overline{u} \gamma_\mu (1 - \gamma_5) q], \quad (2.36)$$

we obtain

$$\langle \bar{u}_q | (\bar{q}_\alpha u_\alpha)_{V-A} | 0 \rangle = -e^{i\phi_{\text{CP}}(u_q)} \langle u_q | (\bar{u}_\alpha q_\alpha)_{V-A} | 0 \rangle \quad (2.37)$$

$$\langle \bar{D}_q | (\bar{q}_\alpha c_\alpha)_{V-A} | 0 \rangle = -e^{i\phi_{\text{CP}}(D_q)} \langle D_q | (\bar{c}_\alpha q_\alpha)_{V-A} | 0 \rangle \quad (2.38)$$

for the pseudoscalar mesons, and

$$\langle \bar{D}_q | (\bar{q}_\alpha c_\alpha)_{V-A} | 0 \rangle = +e^{i\phi_{\text{CP}}(D_q)} \langle D_q | (\bar{c}_\alpha q_\alpha)_{V-A} | 0 \rangle \quad (2.39)$$

for the vector mesons $D_s = D_s^{*+}$ and $D_d = D^{*+}$. If we now use these expressions in (2.33) and (2.34), we see explicitly that the phase-convention-dependent factor in (2.24) is cancelled through the ratio of hadronic matrix elements, thereby yielding a *convention-independent* result. In the case of the decays $B_s \rightarrow D_s^\pm K^\mp$ and $B_d \rightarrow D^\pm \pi^\mp$, we obtain

$$a_s e^{i\delta_s} \Big|_{\text{fact}} = \frac{f_{D_s} F_{B_s K^\pm}^{(0)}(M_{D_s}^2)(M_{B_s}^2 - M_{K^\pm}^2)}{f_{K^\pm} F_{B_s D_s}^{(0)}(M_{K^\pm}^2)(M_{B_s}^2 - M_{D_s}^2)} \quad (2.40)$$

and

$$a_d e^{i\delta_d} \Big|_{\text{fact}} = \frac{f_{D_d} F_{B_d \pi^\pm}^{(0)}(M_{D_d}^2)(M_{B_d}^2 - M_{\pi^\pm}^2)}{f_{\pi^\pm} F_{B_d D_d}^{(0)}(M_{\pi^\pm}^2)(M_{B_d}^2 - M_{D_d}^2)}, \quad (2.41)$$

respectively. If we apply heavy-quark arguments to the $\bar{B}_s^0 \rightarrow D_s^+ K^-$ and $\bar{B}_d^0 \rightarrow D^+ \pi^-$ modes [21, 23], we arrive at

$$a_s e^{i\delta_s} \Big|_{\text{fact}} = \frac{2f_{D_s} F_{B_s K^\pm}^{(0)}(M_{D_s}^2)(M_{B_s}^2 - M_{K^\pm}^2)\sqrt{M_{B_s} M_{D_s}}}{f_{K^\pm} \xi_s(w_s)(M_{B_s} - M_{D_s})[(M_{B_s} + M_{D_s})^2 - M_{K^\pm}^2]} \quad (2.42)$$

$$a_d e^{i\delta_d} \Big|_{\text{fact}} = \frac{2f_{D_d} F_{B_d \pi^\pm}^{(0)}(M_{D_d}^2)(M_{B_d}^2 - M_{\pi^\pm}^2)\sqrt{M_{B_d} M_{D_d}}}{f_{\pi^\pm} \xi_d(w_d)(M_{B_d} - M_{D_d})[(M_{B_d} + M_{D_d})^2 - M_{\pi^\pm}^2]}, \quad (2.43)$$

where the $\xi_q(w_q)$ are the Isgur–Wise functions describing $\bar{B}_q^0 \rightarrow D_q$ transitions, and

$$w_s = \frac{M_{B_s}^2 + M_{D_s}^2 - M_{K^\pm}^2}{2M_{B_s} M_{D_s}}, \quad w_d = \frac{M_{B_d}^2 + M_{D_d}^2 - M_{\pi^\pm}^2}{2M_{B_d} M_{D_d}}. \quad (2.44)$$

In the case of $B_s \rightarrow D_s^{*\pm} K^\mp$ and $B_d \rightarrow D^{*\pm} \pi^\mp$, we obtain accordingly

$$a_{s*} e^{i\delta_{s*}} \Big|_{\text{fact}} = -\frac{f_{D_s^*} F_{B_s K^\pm}^{(1)}(M_{D_s^*}^2)}{f_{K^\pm} A_{B_s D_s^*}^{(0)}(M_{K^\pm}^2)} = -\frac{2f_{D_s^*} F_{B_s K^\pm}^{(1)}(M_{D_s^*}^2)\sqrt{M_{B_s} M_{D_s^*}}}{f_{K^\pm} \xi_s(w_s^*)(M_{B_s} + M_{D_s^*})} \quad (2.45)$$

and

$$a_{d*} e^{i\delta_{d*}} \Big|_{\text{fact}} = -\frac{f_{D_d^*} F_{B_d \pi^\pm}^{(1)}(M_{D_d^*}^2)}{f_{\pi^\pm} A_{B_d D_d^*}^{(0)}(M_{\pi^\pm}^2)} = -\frac{2f_{D_d^*} F_{B_d \pi^\pm}^{(1)}(M_{D_d^*}^2)\sqrt{M_{B_d} M_{D_d^*}}}{f_{\pi^\pm} \xi_d(w_d^*)(M_{B_d} + M_{D_d^*})}, \quad (2.46)$$

respectively, where we have taken the relative minus sign between (2.37) and (2.39) into account, and

$$w_s^* = \frac{M_{B_s}^2 + M_{D_s^*}^2 - M_{K^\pm}^2}{2M_{B_s}M_{D_s^*}}, \quad w_d^* = \frac{M_{B_d}^2 + M_{D_d^*}^2 - M_{\pi^\pm}^2}{2M_{B_d}M_{D_d^*}}. \quad (2.47)$$

An important result of this exercise is

$$\delta_q|_{\text{fact}} = 0^\circ, \quad \delta_{q^*}|_{\text{fact}} = 180^\circ. \quad (2.48)$$

Since factorization is expected to work well for $\overline{B}_q^0 \rightarrow D_q \overline{u}_q$, in contrast to $\overline{B}_q^0 \rightarrow \overline{D}_q u_q$, (2.48) may in principle receive large corrections, yielding sizeable CP-conserving strong phases. However, we may argue that we still have

$$\cos \delta_q > 0, \quad \cos \delta_{q^*} < 0, \quad (2.49)$$

in accordance with the factorization prediction. This valuable information allows us to fix the sign of $\sin(\phi_q + \gamma)$ from (2.31), where the $(-1)^L$ factor plays an important rôle, as we already noted: it is $+1$ and -1 for $B_s \rightarrow D_s^\pm K^\mp$, $B_d \rightarrow D^\pm \pi^\mp$ and $B_s \rightarrow D_s^{*\pm} K^\mp$, $B_d \rightarrow D^{*\pm} \pi^\mp$, respectively. Moreover, it should not be forgotten in this context that x_s is positive, whereas x_d is *negative* because of a factor of -1 originating from the ratio of CKM factors v_d/\overline{v}_d^* (see (2.23)).

Using, for instance, the Bauer–Stech–Wirbel form factors [24], we obtain $a_d = 0.8$ and $a_{d^*} = 1.0$; if we take also (2.9) and (2.23) into account, these values can be converted into $x_{d(*)} = \mathcal{O}(-0.02)$, whereas $x_{s(*)} = \mathcal{O}(0.4)$. In Section 6, we shall have a closer look at the flavour-symmetry-breaking effects, which arise in the ratios a_s/a_d and a_{s^*}/a_{d^*} .

It is useful to briefly compare these results with the situation of the colour-suppressed counterparts of the $B_q \rightarrow D_q \overline{u}_q$ decays, the $B_s \rightarrow D\eta^{(\prime)}, D\phi, \dots$ and $B_d \rightarrow D\pi^0, D\rho^0, \dots$ modes discussed in [16, 17]. Here factorization may receive sizeable corrections for each of the $B_q^0 \rightarrow D^0 f_q$ and $\overline{B}_q^0 \rightarrow D^0 \overline{f}_q$ amplitudes. However, the corresponding hadronic matrix elements are actually very similar to one another, so that the factorized matrix elements cancel in the counterpart of $a_q e^{i\delta_q}$. Consequently, the thus obtained information on the sign of the cosine of the corresponding strong phase difference δ_{f_q} appears to be a bit more robust than (2.49).

3 Conventional Extraction of $\phi_q + \gamma$

We are now well prepared to discuss the “conventional” extraction of the CP-violating phase $\phi_q + \gamma$ from $B_q \rightarrow D_q \overline{u}_q$ decays [11, 12]. As we have already noted, because of (2.28), it is obvious that these modes and their CP conjugates provide a theoretically clean extraction of this phase. Using (2.30), we may – in principle – determine x_q through

$$x_q = \eta_q \sqrt{\frac{1 - \langle C_q \rangle_-}{1 + \langle C_q \rangle_-}}, \quad (3.1)$$

where

$$\eta_q = \begin{cases} +1 & (q = s) \\ -1 & (q = d) \end{cases} \quad (3.2)$$

takes into account the minus sign appearing in (2.23) for $q = d$. Using the knowledge of x_q , we may extract the following quantities from the combinations of the mixing-induced observables introduced in (2.31) and (2.32):

$$s_+ \equiv (-1)^L \left[\frac{1 + x_q^2}{2 x_q} \right] \langle S_q \rangle_+ = + \cos \delta_q \sin(\phi_q + \gamma) \quad (3.3)$$

$$s_- \equiv (-1)^L \left[\frac{1 + x_q^2}{2 x_q} \right] \langle S_q \rangle_- = - \sin \delta_q \cos(\phi_q + \gamma), \quad (3.4)$$

which allow us to determine $\sin^2(\phi_q + \gamma)$ with the help of

$$\sin^2(\phi_q + \gamma) = \frac{1}{2} \left[(1 + s_+^2 - s_-^2) \pm \sqrt{(1 + s_+^2 - s_-^2)^2 - 4 s_+^2} \right]. \quad (3.5)$$

This relation implies a fourfold solution for $\sin(\phi_q + \gamma)$. Since each value of this quantity corresponds to a twofold solution for $\phi_q + \gamma$, the extraction of this phase suffers, in general, from an eightfold discrete ambiguity. If we employ (2.49) and (3.3), the measured sign of s_+ allows us to fix the sign of $\sin(\phi_q + \gamma)$, thereby reducing the discrete ambiguity for the value of $\phi_q + \gamma$ to a fourfold one. Needless to note that these unpleasant ambiguities significantly reduce the power to search for possible signals of new physics.

Another disadvantage is that the determination of the hadronic parameter x_q through (3.1) requires the experimental resolution of small x_q^2 terms in (2.30). In the $q = s$ case, we naïvely expect $x_s^2 = \mathcal{O}(0.16)$, so that this may actually be possible, though challenging.¹ On the other hand, it is practically impossible to resolve the $x_d^2 = \mathcal{O}(0.0004)$ terms, i.e. (2.30) is not effective in the $q = d$ case. However, it may well be possible to measure the observable combinations $\langle S_d \rangle_+$ and $\langle S_d \rangle_-$, since these quantities are proportional to $x_d = \mathcal{O}(-0.02)$. In this respect, $B_d \rightarrow D^{*\pm} \pi^\mp$ channels are particularly promising, since they exhibit large branching ratios at the 10^{-3} level and offer a good reconstruction of the $D^{*\pm} \pi^\mp$ states with a high efficiency and modest backgrounds [25, 26]. In order to solve the problem of the extraction of x_d , which was also addressed in [12], we shall propose the use of “untagged” decay rates, where we do not distinguish between initially, i.e. at time $t = 0$, present B_d^0 or \overline{B}_d^0 mesons. Also in the case of $q = s$, alternatives to (3.1) for an efficient determination of x_s are obviously desirable.

¹Note that non-factorizable effects may well lead to a significant reduction or enhancement of x_s .

4 Closer Look at “Untagged” Rates

4.1 New Strategy Employing $\Delta\Gamma_q$

As we have seen in (2.18), the width difference $\Delta\Gamma_q$ of the B_q mass eigenstates provides another observable, $\mathcal{A}_{\Delta\Gamma}(B_q \rightarrow D_q \bar{u}_q)$, which is given by

$$\mathcal{A}_{\Delta\Gamma}(B_q \rightarrow D_q \bar{u}_q) = \frac{2 \operatorname{Re} \xi_q}{1 + |\xi_q|^2}. \quad (4.1)$$

This quantity is, however, not independent from $C(B_q \rightarrow D_q \bar{u}_q)$ and $S(B_q \rightarrow D_q \bar{u}_q)$, satisfying the relation

$$\left[C(B_q \rightarrow D_q \bar{u}_q) \right]^2 + \left[S(B_q \rightarrow D_q \bar{u}_q) \right]^2 + \left[\mathcal{A}_{\Delta\Gamma}(B_q \rightarrow D_q \bar{u}_q) \right]^2 = 1. \quad (4.2)$$

Interestingly, $\mathcal{A}_{\Delta\Gamma}(B_q \rightarrow D_q \bar{u}_q)$ could be determined from the “untagged” rate

$$\begin{aligned} \langle \Gamma(B_q(t) \rightarrow D_q \bar{u}_q) \rangle &\equiv \Gamma(B_q^0(t) \rightarrow D_q \bar{u}_q) + \Gamma(\bar{B}_q^0(t) \rightarrow D_q \bar{u}_q) \\ &= \left[\Gamma(B_q^0 \rightarrow D_q \bar{u}_q) + \Gamma(\bar{B}_q^0 \rightarrow D_q \bar{u}_q) \right] \\ &\quad \times [\cosh(\Delta\Gamma_q t/2) - \mathcal{A}_{\Delta\Gamma}(B_q \rightarrow D_q \bar{u}_q) \sinh(\Delta\Gamma_q t/2)] e^{-\Gamma_q t}, \end{aligned} \quad (4.3)$$

where the oscillatory $\cos(\Delta M_q t)$ and $\sin(\Delta M_q t)$ terms cancel, and $\Gamma_q \equiv (\Gamma_H^{(q)} + \Gamma_L^{(q)})/2$ denotes the average decay width [27]. In the case of the B_d -meson system, the width difference is negligibly small, so that the time evolution of (4.3) is essentially given by the well-known exponential $e^{-\Gamma_d t}$. On the other hand, the width difference $\Delta\Gamma_s$ of the B_s -meson system may be as large as $\mathcal{O}(-10\%)$ (for a recent review, see [28]), and may hence allow us to extract $\mathcal{A}_{\Delta\Gamma}(B_s \rightarrow D_s \bar{u}_s)$.

Inserting (2.22) into (4.1), we obtain

$$\mathcal{A}_{\Delta\Gamma}(B_s \rightarrow D_s \bar{u}_s) \equiv \mathcal{A}_{\Delta\Gamma_s} = -(-1)^L \left[\frac{2 x_s \cos(\phi_s + \gamma + \delta_s)}{1 + x_s^2} \right], \quad (4.4)$$

and correspondingly

$$\mathcal{A}_{\Delta\Gamma}(B_s \rightarrow \bar{D}_s u_s) \equiv \bar{\mathcal{A}}_{\Delta\Gamma_s} = -(-1)^L \left[\frac{2 x_s \cos(\phi_s + \gamma - \delta_s)}{1 + x_s^2} \right], \quad (4.5)$$

which yields

$$\langle \mathcal{A}_{\Delta\Gamma_s} \rangle_+ \equiv \frac{\bar{\mathcal{A}}_{\Delta\Gamma_s} + \mathcal{A}_{\Delta\Gamma_s}}{2} = -(-1)^L \left[\frac{2 x_s \cos \delta_s}{1 + x_s^2} \right] \cos(\phi_s + \gamma) \quad (4.6)$$

$$\langle \mathcal{A}_{\Delta\Gamma_s} \rangle_- \equiv \frac{\bar{\mathcal{A}}_{\Delta\Gamma_s} - \mathcal{A}_{\Delta\Gamma_s}}{2} = -(-1)^L \left[\frac{2 x_s \sin \delta_s}{1 + x_s^2} \right] \sin(\phi_s + \gamma). \quad (4.7)$$

If we compare now (4.6) and (4.7) with (2.31) and (2.32), respectively, we observe that the same hadronic factors enter in these mixing-induced observables, and obtain

$$\frac{\langle S_s \rangle_+}{\langle \mathcal{A}_{\Delta\Gamma_s} \rangle_+} = -\tan(\phi_s + \gamma) \quad (4.8)$$

$$\frac{\langle \mathcal{A}_{\Delta\Gamma_s} \rangle_-}{\langle S_s \rangle_-} = +\tan(\phi_s + \gamma), \quad (4.9)$$

implying the consistency relation

$$\langle \mathcal{A}_{\Delta\Gamma_s} \rangle_+ \langle \mathcal{A}_{\Delta\Gamma_s} \rangle_- = -\langle S_s \rangle_+ \langle S_s \rangle_-. \quad (4.10)$$

Should δ_s take values around 0° or 180° , as in factorization (see (2.48)), we may extract $\tan(\phi_s + \gamma)$ from (4.8), whereas we could use (4.9) in the opposite case of δ_s being close to $+90^\circ$ or -90° . The strong phase itself can be determined from

$$\tan \delta_s = \frac{\langle S_s \rangle_-}{\langle \mathcal{A}_{\Delta\Gamma_s} \rangle_+} = -\frac{\langle \mathcal{A}_{\Delta\Gamma_s} \rangle_-}{\langle S_s \rangle_+}. \quad (4.11)$$

The values of $\tan(\phi_s + \gamma)$ and $\tan \delta_s$ thus extracted imply twofold solutions for $\phi_s + \gamma$ and δ_s , respectively, which should be compared with the eightfold solution for $\phi_s + \gamma$ following from (3.5). Using (2.49), we may immediately fix δ_s unambiguously, and may determine the sign of $\sin(\phi_s + \gamma)$ with the help of the measured sign of $\langle S_s \rangle_+$ from (2.31), thereby resolving the twofold ambiguity for the value of $\phi_s + \gamma$. On the other hand, the “conventional” approach discussed in Section 3 would still leave a fourfold ambiguity for this phase, as we shall illustrate in Section 5. Finally, we may of course also determine x_s from one of the $\langle S_s \rangle_\pm$ or $\langle \mathcal{A}_{\Delta\Gamma_s} \rangle_\pm$ observables.

We observe that the combination of the “tagged” mixing-induced observables $\langle S_s \rangle_\pm$ with their “untagged” counterparts $\langle \mathcal{A}_{\Delta\Gamma_s} \rangle_\pm$ provides an elegant determination of $\phi_s + \gamma$ in an essentially unambiguous manner. In [13], strategies to determine this phase from untagged B_s data samples only were proposed, which employ angular distributions of decays of the kind $B_s \rightarrow D_s^{*\pm} K^{*\mp}$ and are hence considerably more involved. Another important advantage of our new strategy is that both $\langle S_s \rangle_\pm$ and $\langle \mathcal{A}_{\Delta\Gamma_s} \rangle_\pm$ are proportional to x_s . Consequently, the extraction of $\phi_s + \gamma$ does not require the resolution of x_s^2 terms.² On the other hand, we have to rely on a sizeable width difference $\Delta\Gamma_s$, which may be too small to make an extraction of $\langle \mathcal{A}_{\Delta\Gamma_s} \rangle_\pm$ experimentally feasible. In the presence of CP-violating new-physics contributions to $B_s^0 - \overline{B}_s^0$ mixing, manifesting themselves through a sizeable value of ϕ_s , $\Delta\Gamma_s$ would be further reduced, as follows [29]:

$$\Delta\Gamma_s = \Delta\Gamma_s^{\text{SM}} \cos \phi_s, \quad (4.12)$$

where $\Delta\Gamma_s^{\text{SM}}$ is negative [28]. As is well known, ϕ_s can be determined through $B_s \rightarrow J/\psi\phi$, which is very accessible at hadronic B -decay experiments [25, 30]. Strategies to determine ϕ_s *unambiguously* were proposed in [9, 16].

²A similar feature is also present in the “untagged” $B_s \rightarrow D_s^{*\pm} K^{*\mp}$ strategy proposed in [13], and in the “tagged” analysis in [14], employing the angular distribution of the $D_s^{*\pm}$, $K^{*\mp}$ decay products.

In the case of the $B_s \rightarrow D\eta^{(\prime)}, D\phi, \dots$ modes – the colour-suppressed counterparts of the $B_s \rightarrow D_s \bar{u}_s$ channels, untagged rates for processes where the neutral D mesons are observed through their decays into CP eigenstates f_{\pm} provide a very useful “untagged” rate asymmetry Γ_{\pm} , allowing efficient and essentially unambiguous determinations of γ from mixing-induced observables [16, 17]. These strategies, which can also be implemented for $B_d \rightarrow DK_{S(L)}$ modes, have certain similarities with those provided by (4.8) and (4.9). However, they do not rely on a sizeable value of $\Delta\Gamma_q$, as Γ_{\pm} is extracted from “unevolved” untagged rates, which are also very useful for the analysis of $B_q \rightarrow D_q \bar{u}_q$ modes, as we shall see below. Since these decays involve charged D_q mesons, the Γ_{\pm} observable has unfortunately no counterpart for the colour-allowed transitions.

4.2 Employing Untagged Rates in the Case of Negligible $\Delta\Gamma_q$

Even for a vanishingly small width difference $\Delta\Gamma_q$, the untagged rate (4.3) provides valuable information, as it still allows us to determine the “unevolved”, untagged rate

$$\langle \Gamma(B_q \rightarrow D_q \bar{u}_q) \rangle \equiv \Gamma(B_q^0 \rightarrow D_q \bar{u}_q) + \Gamma(\bar{B}_q^0 \rightarrow D_q \bar{u}_q). \quad (4.13)$$

Using (2.1) and (2.14), as well as (2.16) and (2.17), we obtain

$$\frac{\langle \Gamma(B_q \rightarrow D_q \bar{u}_q) \rangle}{\Gamma(B_q^0 \rightarrow D_q \bar{u}_q)} = 1 + \frac{1}{x_q^2} = \frac{\langle \Gamma(B_q \rightarrow \bar{D}_q u_q) \rangle}{\Gamma(\bar{B}_q^0 \rightarrow \bar{D}_q u_q)}. \quad (4.14)$$

If we now employ

$$\Gamma(B_q^0 \rightarrow D_q \bar{u}_q) = \Gamma(\bar{B}_q^0 \rightarrow \bar{D}_q u_q), \quad (4.15)$$

which follows from (2.14) and (2.16), we may write

$$x_q = \eta_q \left[\frac{\langle \Gamma(B_q \rightarrow D_q \bar{u}_q) \rangle + \langle \Gamma(B_q \rightarrow \bar{D}_q u_q) \rangle}{\Gamma(B_q^0 \rightarrow D_q \bar{u}_q) + \Gamma(\bar{B}_q^0 \rightarrow \bar{D}_q u_q)} - 1 \right]^{-\frac{1}{2}}, \quad (4.16)$$

offering a very attractive “untagged” alternative to (3.1), provided we fix the sum of the $B_q^0 \rightarrow D_q \bar{u}_q$ rate and its CP conjugate in an efficient manner. To this end, we may replace the spectator quark q by an up quark, which will allow us to determine this quantity from the CP-averaged rate of a charged B -meson decay as follows:³

$$\Gamma(B_q^0 \rightarrow D_q \bar{u}_q) + \Gamma(\bar{B}_q^0 \rightarrow \bar{D}_q u_q) = 2\mathcal{C}_q^2 \left[\Gamma(B^+ \rightarrow D_q \bar{u}_u) + \Gamma(B^- \rightarrow \bar{D}_q u_u) \right], \quad (4.17)$$

where $u_u \in \{\pi^0, \rho^0, \dots\}$ depends on the choice of u_q . For example, we have $u_u = \pi^0$ for $u_d = \pi^+$ or $u_s = K^+$, whereas $u_u = \rho^0$ for $u_d = \rho^+$ or $u_s = K^{*+}$. The factor of 2 takes into account the $1/\sqrt{2}$ factor of the u_u wave function, and the deviation of \mathcal{C}_q from 1 is governed by flavour-symmetry-breaking effects, which originate from the replacement of the spectator quark q through an up quark.

³For simplicity, we neglect tiny phase-space effects, which can be straightforwardly included.

Since $B^+ \rightarrow D_d \bar{u}_u$ is related to $B_d^0 \rightarrow D_d \bar{u}_d$ through $SU(2)$ isospin arguments, we obtain to a good approximation

$$\mathcal{C}_d = 1. \quad (4.18)$$

In addition to the “conventional” isospin-breaking effects, exchange topologies, which contribute to $B_d^0 \rightarrow D_d \bar{u}_d$ but have no counterpart in $B^+ \rightarrow D_d \bar{u}_u$, and annihilation topologies, which arise only in $B^+ \rightarrow D_d \bar{u}_u$ but not in $B_d^0 \rightarrow D_d \bar{u}_d$, are another limiting factor of the theoretical accuracy of (4.18). Although these contributions are naïvely expected to be very small, they may – in principle – be enhanced through rescattering processes. Fortunately, we may probe their importance experimentally. In the case of $B_d \rightarrow D^{(*)\pm} \pi^\mp$ and $B^+ \rightarrow D^{(*)+} \pi^0$ this can be done with the help of $B_d \rightarrow D_s^{(*)\pm} K^\mp$ and $B^+ \rightarrow D^{(*)+} K^0$ processes, respectively.

Applying (4.17) to the $q = s$ case, we have to employ the $SU(3)$ flavour symmetry. If we neglect non-factorizable $SU(3)$ -breaking effects, the \mathcal{C}_s are simply given by appropriate form-factor ratios; important examples are the following ones:

$$B_s \rightarrow D_s^\pm K^\mp : \frac{F_{B_s K^\pm}^{(0)}(M_{D_s}^2)(M_{B_s}^2 - M_{K^\pm}^2)}{F_{B^\pm \pi^0}^{(0)}(M_{D_s}^2)(M_{B_u}^2 - M_{\pi^\pm}^2)}, \quad B_s \rightarrow D_s^{*\pm} K^\mp : \frac{F_{B_s K^\pm}^{(1)}(M_{D_s^*}^2)}{F_{B^\pm \pi^0}^{(1)}(M_{D_s^*}^2)}. \quad (4.19)$$

Also here, we have to deal with exchange topologies, which contribute to $B_s^0 \rightarrow D_s^{(*)+} K^-$ but have no counterpart in $B^+ \rightarrow D_s^{(*)+} \pi^0$. Experimental probes for these topologies are provided by $B_s \rightarrow D^{(*)\pm} \pi^\mp$ processes.

As an alternative to (4.17), we may use

$$\Gamma(B_d^0 \rightarrow D^{(*)+} \pi^-) + \Gamma(\bar{B}_d^0 \rightarrow D^{(*)-} \pi^+) = \zeta \left[\Gamma(B_d^0 \rightarrow D_s^{(*)+} \pi^-) + \Gamma(\bar{B}_d^0 \rightarrow D_s^{(*)-} \pi^+) \right] \quad (4.20)$$

and

$$\Gamma(B_s^0 \rightarrow D_s^{(*)+} K^-) + \Gamma(\bar{B}_s^0 \rightarrow D_s^{(*)-} K^+) = \frac{1}{\zeta} \left[\Gamma(B_s^0 \rightarrow D^{(*)+} K^-) + \Gamma(\bar{B}_s^0 \rightarrow D^{(*)-} K^+) \right], \quad (4.21)$$

where

$$\zeta \equiv \left(\frac{\lambda^2}{1 - \lambda^2} \right) \left[\frac{f_{D_d^{(*)}}}{f_{D_s^{(*)}}} \right]^2 \quad (4.22)$$

takes into account factorizable $SU(3)$ -breaking corrections through the ratio of the $D_d^{(*)}$ and $D_s^{(*)}$ decay constants. The decays on the right-hand sides of (4.20) and (4.21) have the advantage of involving “flavour-specific” final states f , satisfying $A(B_q^0 \rightarrow f) \neq 0$ and $A(\bar{B}_q^0 \rightarrow f) = 0$. In this important special case, the time-dependent untagged rates take the following simple forms:

$$\langle \Gamma(B_q(t) \rightarrow f) \rangle \equiv \Gamma(B_q^0(t) \rightarrow f) + \Gamma(\bar{B}_q^0(t) \rightarrow f) = \Gamma(B_q^0 \rightarrow f) \cosh(\Delta\Gamma_q t/2) e^{-\Gamma_q t} \quad (4.23)$$

$$\langle \Gamma(B_q(t) \rightarrow \bar{f}) \rangle \equiv \Gamma(B_q^0(t) \rightarrow \bar{f}) + \Gamma(\bar{B}_q^0(t) \rightarrow \bar{f}) = \Gamma(\bar{B}_q^0 \rightarrow \bar{f}) \cosh(\Delta\Gamma_q t/2) e^{-\Gamma_q t}, \quad (4.24)$$

and allow an efficient extraction of the CP-averaged rate $\Gamma(B_q^0 \rightarrow f) + \Gamma(\overline{B}_q^0 \rightarrow \overline{f})$ with the help of

$$\langle \Gamma(B_q(t) \rightarrow f) \rangle + \langle \Gamma(B_q(t) \rightarrow \overline{f}) \rangle = \left[\Gamma(B_q^0 \rightarrow f) + \Gamma(\overline{B}_q^0 \rightarrow \overline{f}) \right] \cosh(\Delta\Gamma_q t/2) e^{-\Gamma_q t}. \quad (4.25)$$

Obviously, in the case of $q = d$, (4.17) is theoretically cleaner than (4.20), providing – in combination with (4.16) – a very interesting avenue to determine x_d . On the other hand, the modes on the right-hand side of (4.20) are more accessible from an experimental point of view, and were already observed at the B factories [31].

Since simple colour-transparency arguments do not apply to $B_q^0 \rightarrow D_q \overline{u}_q$, $B^+ \rightarrow D_q \overline{u}_q$ modes, as we noted in Subsection 2.3, expressions (4.19), (4.20) and (4.21) may receive sizeable non-factorizable $SU(3)$ -breaking corrections. However, there is yet another possibility to exploit (4.13). To this end, we factor out the $B_q^0 \rightarrow \overline{D}_q u_q$ rate, where factorization is expected to work well [22], yielding

$$\frac{\langle \Gamma(B_q \rightarrow D_q \overline{u}_q) \rangle}{\Gamma(\overline{B}_q^0 \rightarrow D_q \overline{u}_q)} = 1 + x_q^2 = \frac{\langle \Gamma(B_q \rightarrow \overline{D}_q u_q) \rangle}{\Gamma(B_q^0 \rightarrow \overline{D}_q u_q)}, \quad (4.26)$$

which implies

$$x_q = \eta_q \sqrt{\frac{\langle \Gamma(B_q \rightarrow D_q \overline{u}_q) \rangle + \langle \Gamma(B_q \rightarrow \overline{D}_q u_q) \rangle}{\Gamma(\overline{B}_q^0 \rightarrow D_q \overline{u}_q) + \Gamma(B_q^0 \rightarrow \overline{D}_q u_q)}} - 1. \quad (4.27)$$

In the $q = d$ case, it will – in analogy to (2.30) – be impossible to resolve the vanishingly small x_q^2 term in (4.26). On the other hand, this may well be possible in the $q = s$ case. If we use

$$\begin{aligned} & \Gamma(\overline{B}_s^0 \rightarrow D_s^{(*)+} K^-) + \Gamma(B_s^0 \rightarrow D_s^{(*)-} K^+) \\ &= \left(\frac{\lambda^2}{1 - \lambda^2} \right) \left(\frac{f_K}{f_\pi} \right)^2 \left[\Gamma(\overline{B}_s^0 \rightarrow D_s^{(*)+} \pi^-) + \Gamma(B_s^0 \rightarrow D_s^{(*)-} \pi^+) \right], \end{aligned} \quad (4.28)$$

expression (4.27) offers a very attractive possibility to determine the values of $x_{s(*)}$, where $(f_K/f_\pi)^2$ describes factorizable $SU(3)$ -breaking effects. Additional corrections are due to exchange topologies, which arise in $\overline{B}_s^0 \rightarrow D_s^{(*)+} K^-$, but are not present in $\overline{B}_s^0 \rightarrow D_s^{(*)+} \pi^-$. However, as we already noted, their contributions are expected to be very small, and can be probed experimentally through $B_s \rightarrow D^{(*)\pm} \pi^\mp$ processes. Since the $\overline{B}_s^0 \rightarrow D_s^{(*)+} \pi^-$ and $B_s^0 \rightarrow D_s^{(*)-} \pi^+$ rates involve flavour-specific final states, we may efficiently determine their sum from untagged B_s data samples, with the help of (4.25). In this context, it should also be noted that these rates are enhanced by a factor of $(1 - \lambda^2)/\lambda^2 \approx 20$ with respect to the $B_s \rightarrow D_s^{(*)\pm} K^\mp$ rates. Moreover, non-factorizable effects are expected to play a minor rôle in (4.28) because of colour-transparency arguments, in contrast to (4.19) and (4.21). Further calculations along [22] should provide an even more accurate treatment of the $SU(3)$ -breaking corrections. In comparison with (3.1), the advantage of the strategy offered by (4.27) and (4.28) is the use of untagged rates, which are particularly promising in terms of efficiency, acceptance and purity, and do not require the measurement of the

time-dependent $\cos(\Delta M_s t)$ terms in (2.18). Interestingly, the quantity $1 + x_s^2$, which can nicely be determined through the combination of (4.27) and (4.28), will play an important rôle in Section 6.

As we have seen above, the untagged rates introduced in (4.3) provide various strategies to determine the hadronic parameters x_q , some of which are particularly favourable. In order to implement these approaches, we must not rely on a sizeable width difference $\Delta\Gamma_q$. It will be interesting to see whether they will eventually yield a consistent picture of the x_q . Following these lines, we may also obtain valuable insights into hadron dynamics.

5 Bounds on $\phi_q + \gamma$

If we keep x_q and δ_q as “unknown”, i.e. free parameters in (2.31) and (2.32), we may derive the following bounds:

$$|\sin(\phi_q + \gamma)| \geq |\langle S_q \rangle_+| \quad (5.1)$$

$$|\cos(\phi_q + \gamma)| \geq |\langle S_q \rangle_-|. \quad (5.2)$$

On the other hand, if we assume that x_q has been determined with the help of the “untagged” strategies proposed in Subsection 4.2, we may fix the quantities s_+ and s_- introduced in (3.3) and (3.4), respectively, providing more stringent constraints:

$$|\sin(\phi_q + \gamma)| \geq |s_+| \quad (5.3)$$

$$|\cos(\phi_q + \gamma)| \geq |s_-|. \quad (5.4)$$

Interestingly, (5.1) and (5.3) allow us to exclude a certain range of values of $\phi_q + \gamma$ around 0° and 180° , whereas (5.2) and (5.4) provide complementary information, excluding a certain range around 90° and 270° . The constraints in (5.1) and (5.2) have the advantage of not requiring knowledge of x_q . On the other hand, because of the small value of x_d , we may only expect useful information from them in the case of $q = s$. Once s_+ and s_- have been extracted, it is of course also possible to determine $\sin^2(\phi_q + \gamma)$ through the complicated expression in (3.5), as discussed in Section 3. However, since the resulting values for $\phi_q + \gamma$ suffer from multiple discrete ambiguities, the information they are expected to provide about this phase is – in general – not significantly better than the constraints following from the very simple relations in (5.3) and (5.4).

It is instructive to illustrate this feature with the help of a few numerical examples. To this end, we assume $\gamma = 60^\circ$, $\phi_d = 47^\circ$ and $\phi_s = 0^\circ$, which would be in perfect agreement with the Standard Model, as well as $R_b = 0.4$ and $a_q = 1$. Let us consider the decays $B_d \rightarrow D^\pm \pi^\mp$ and $B_s \rightarrow D_s^\pm K^\mp$, which have $L = 0$. As far as δ_q is concerned, we may then distinguish between a “factorization” scenario with $\delta_q = 0^\circ$ (see (2.48)), and a “non-factorization” scenario, corresponding to $\delta_q = 40^\circ$. For simplicity, we shall use the same hadronic parameters $a_q e^{i\delta_q}$ for the $q = d$ and $q = s$ cases. The corresponding mixing-induced observables are listed in Table 1. Let us also assume that ϕ_d and ϕ_s will be unambiguously known by the time these observables can be measured. As we have

q	S_q	\bar{S}_q	$\langle S_q \rangle_+$	$\langle S_q \rangle_-$	s_+	s_-
d	-3.89%	-3.89%	-3.89%	+0.00%	+95.6%	+0.00%
s	+59.7%	+59.7%	+59.7%	+0.00%	+86.6%	+0.00%
d	-2.22%	-3.74%	-2.98%	-0.76%	+73.3%	+18.8%
s	+67.9%	+23.6%	+45.8%	-22.2%	+66.3%	-32.1%

Table 1: The mixing-induced observables in the case of $L = 0$, $\gamma = 60^\circ$, $\phi_d = 47^\circ$, $\phi_s = 0^\circ$, $R_b = 0.4$ and $a_q = 1$: the upper half corresponds to factorization, i.e. $\delta_q = 0^\circ$, whereas the lower half illustrates a non-factorization scenario with $\delta_q = 40^\circ$. Note that we have $\langle C_s \rangle_- = 0.724$, while the deviation of $\langle C_d \rangle_-$ from 1 is negligibly small.

already noted, because of the small value of x_d , (5.1) and (5.2) do not provide non-trivial constraints on $\phi_d + \gamma$, in contrast to their application to the $q = s$ case.

Let us first focus on the factorization scenario, corresponding to the upper half of Table 1. Since $\langle S_q \rangle_-$ and s_- vanish in this case, as these observable combinations are proportional to $\sin \delta_q$, (5.2) and (5.4) imply only trivial constraints on $\phi_q + \gamma$. However, we may nevertheless obtain interesting bounds in this case. For the $q = d$ example, the situation is as follows: if we employ (2.49) and take into account that x_d is negative, the negative sign of $\langle S_d \rangle_+$ implies a positive value of $\sin(\phi_d + \gamma)$, i.e. $0^\circ \leq \phi_d + \gamma \leq 180^\circ$. Applying now (5.3), we obtain $73^\circ \leq \phi_d + \gamma \leq 107^\circ$ from s_+ , which corresponds to $26^\circ \leq \gamma \leq 60^\circ$, providing valuable information about γ . On the other hand, if we use again that $\sin(\phi_d + \gamma)$ is positive, the complicated expression (3.5) implies the threefold solution $\gamma = 26^\circ \vee 43^\circ \vee 60^\circ$, which covers essentially the whole range following from the simple relation in (5.3). It is very interesting to complement the information on γ thus obtained from $B_d \rightarrow D^\pm \pi^\mp$ with the one provided by its $B_s \rightarrow D_s^\pm K^\mp$ counterpart. Using again (2.49), the positive sign of $\langle S_s \rangle_+$ implies that $\sin(\phi_s + \gamma)$ is positive, i.e. $0^\circ \leq \phi_s + \gamma \leq 180^\circ$. We may now apply (5.1) to obtain the bound $37^\circ \leq \phi_s + \gamma \leq 143^\circ$ from $\langle S_s \rangle_+$; a narrower range follows from s_+ through (5.3), and is given by $60^\circ \leq \phi_s + \gamma \leq 120^\circ$. Since $\phi_s = 0^\circ$, we may identify these ranges directly with bounds on γ . On the other hand, the complicated expression (3.5) implies the threefold solution $\gamma = 60^\circ \vee 90^\circ \vee 120^\circ$, which falls perfectly into the range provided by s_+ , which can be obtained in a much simpler manner. We now make the very interesting observation that the $q = s$ range of $60^\circ \leq \gamma \leq 120^\circ$ is highly complementary to its $q = d$ counterpart of $26^\circ \leq \gamma \leq 60^\circ$, leaving 60° as the only overlap. Consequently, in this example, the combination of our simple bounds on $\phi_d + \gamma$ and $\phi_s + \gamma$ yields the single solution of $\gamma = 60^\circ$, which corresponds to our input value, thereby nicely demonstrating the potential power of these constraints.

Let us now perform the same exercise for the non-factorization scenario, represented by the lower half of Table 1. In the case of $q = d$, s_+ and s_- imply $47^\circ \leq \phi_d + \gamma \leq 133^\circ$ and $(0^\circ \leq \phi_d + \gamma \leq 79^\circ) \vee (101^\circ \leq \phi_d + \gamma \leq 180^\circ)$, respectively, which can be combined with each other, taking also $\phi_d = 47^\circ$ into account, to obtain $(0^\circ \leq \gamma \leq 32^\circ) \vee (54^\circ \leq \gamma \leq 86^\circ)$. On the other hand, if we apply (3.5) and use that $\sin(\phi_d + \gamma)$ is positive, we obtain the fourfold solution $\gamma = 3^\circ \vee 26^\circ \vee 60^\circ \vee 83^\circ$. Let us now consider the $q = s$ case. Here $\langle S_s \rangle_+$

and $\langle S_s \rangle_-$ imply $27^\circ \leq \phi_s + \gamma \leq 153^\circ$ and $(0^\circ \leq \phi_s + \gamma \leq 77^\circ) \vee (103^\circ \leq \phi_s + \gamma \leq 180^\circ)$, respectively, yielding the combined range $(27^\circ \leq \phi_s + \gamma \leq 77^\circ) \vee (103^\circ \leq \phi_s + \gamma \leq 153^\circ)$. Using s_+ and s_- , and taking into account that $\phi_s = 0^\circ$, we obtain the more stringent constraint $(42^\circ \leq \gamma \leq 71^\circ) \vee (109^\circ \leq \gamma \leq 138^\circ)$, whereas (3.5) would imply the fourfold solution $\gamma = 50^\circ \vee 60^\circ \vee 120^\circ \vee 130^\circ$, providing essentially the same information. We observe again that the bounds on γ arising in the $q = d$ and $q = s$ cases are highly complementary to each other, having a small overlap of $54^\circ \leq \gamma \leq 71^\circ$. Although the constraint on γ following from the bounds on $\phi_q + \gamma$ would now not be as sharp as in the factorization scenario discussed above, this approach would still provide very non-trivial information about this particularly important angle of the unitarity triangle.

In Table 1, we have considered a Standard-Model-like scenario for the weak phases. However, as argued in [6], the present data are also perfectly consistent with the picture of $(\phi_d, \gamma) = (133^\circ, 120^\circ)$, corresponding to new-physics contributions to $B_d^0 - \overline{B}_d^0$ mixing. Since we have $\sin(\phi_d + \gamma) \rightarrow -\sin(\phi_d + \gamma)$ for $\phi_d \rightarrow 180^\circ - \phi_d$, $\gamma \rightarrow 180^\circ - \gamma$, the sign of the $(-1)^L \langle S_d \rangle_+$ observable combination allows us to distinguish between the $(\phi_d, \gamma) = (47^\circ, 60^\circ)$ and $(133^\circ, 120^\circ)$ scenarios, corresponding to $\sin(\phi_d + \gamma) = +0.956$ and -0.956 , respectively. Practically, this can be done with the help of $B_d \rightarrow D^{(*)\pm} \pi^\mp$ modes. If we take into account that the $x_{d(*)}$ are negative, include properly the $(-1)^L$ factors and fix the signs of $\cos \delta_{d(*)}$ through (2.49), we find that a positive value of the $\langle S_{d(*)} \rangle_+$ observables would be in favour of the “unconventional” $(\phi_d, \gamma) = (133^\circ, 120^\circ)$ scenario, whereas a negative value would point towards the Standard-Model picture of $(\phi_d, \gamma) = (47^\circ, 60^\circ)$. A first preliminary analysis of $B_d \rightarrow D^{*\pm} \pi^\mp$ by the BaBar collaboration [32] gives

$$\langle S_{d*} \rangle_+ = -0.063 \pm 0.024 (\text{stat.}) \pm 0.017 (\text{syst.}), \quad (5.5)$$

thereby favouring the latter case.

6 Combined Analysis of $B_{s,d} \rightarrow D_{s,d} \overline{u}_{s,d}$ Modes

As we have seen in the previous section, it is very useful to make a simultaneous analysis of $B_s \rightarrow D_s \overline{u}_s$ and $B_d \rightarrow D_d \overline{u}_d$ decays. Let us now further explore this observation. Using (2.31) and (2.32), we may write

$$\left[\frac{a_s \cos \delta_s}{a_d \cos \delta_d} \right] R = -(-1)^{L_s - L_d} \left[\frac{\sin(\phi_d + \gamma)}{\sin(\phi_s + \gamma)} \right] \left[\frac{\langle S_s \rangle_+}{\langle S_d \rangle_+} \right] \quad (6.1)$$

and

$$\left[\frac{a_s \sin \delta_s}{a_d \sin \delta_d} \right] R = -(-1)^{L_s - L_d} \left[\frac{\cos(\phi_d + \gamma)}{\cos(\phi_s + \gamma)} \right] \left[\frac{\langle S_s \rangle_-}{\langle S_d \rangle_-} \right], \quad (6.2)$$

respectively, where

$$R \equiv \left(\frac{1 - \lambda^2}{\lambda^2} \right) \left[\frac{1 + x_d^2}{1 + x_s^2} \right]. \quad (6.3)$$

Using the results derived in Subsection 4.2, we may easily determine the parameter R , where the x_d^2 term is negligibly small, and x_s enters only through $1 + x_s^2$, i.e. a moderate

correction. To be specific, let us consider the $B_s \rightarrow D_s^{(*)\pm} K^\mp$ channels. If we insert (4.28) into (4.27), we arrive at

$$R_{(*)} = \left(\frac{f_K}{f_\pi} \right)^2 \left[\frac{\Gamma(\overline{B}_s^0 \rightarrow D_s^{(*)+} \pi^-) + \Gamma(B_s^0 \rightarrow D_s^{(*)-} \pi^+)}{\langle \Gamma(B_s \rightarrow D_s^{(*)+} K^-) \rangle + \langle \Gamma(B_s \rightarrow D_s^{(*)-} K^+) \rangle} \right], \quad (6.4)$$

where the decay rates can be straightforwardly extracted from untagged B_s data samples with the help of (4.3) and (4.25). As we have emphasized in Subsection 4.2, non-factorizable $SU(3)$ -breaking corrections to this relation are expected to be very small.

If we look at Fig. 1, we see that each $B_s \rightarrow D_s \overline{u}_s$ mode has a counterpart $B_d \rightarrow D_d \overline{u}_d$, which can be obtained from the B_s transition by simply replacing all strange quarks through down quarks; an important example is the $B_s^0 \rightarrow D_s^{(*)+} K^-$, $B_d^0 \rightarrow D^{(*)+} \pi^-$ system. For such decay pairs, we have $L_s = L_d$, and the U -spin flavour symmetry of strong interactions, which relates strange and down quarks in the same manner as ordinary isospin relates up and down quarks, implies the following relations for the corresponding hadronic parameters:⁴

$$a_s = a_d, \quad \delta_s = \delta_d, \quad (6.5)$$

which we may apply in a variety of ways.

Let us first consider a factorization-like scenario, where $\cos \delta_s \approx \pm 1 \approx \cos \delta_d$ and $\langle S_s \rangle_- \approx 0 \approx \langle S_d \rangle_-$ (see Table 1). In this case, (6.2) would not be applicable. However, we may use (6.1) to determine $\tan \gamma$ through

$$\tan \gamma = - \left[\frac{\sin \phi_d - S \sin \phi_s}{\cos \phi_d - S \cos \phi_s} \right]_{\phi_s=0^\circ} - \left[\frac{\sin \phi_d}{\cos \phi_d - S} \right], \quad (6.6)$$

where

$$S|_{U \text{ spin}} = -R \left[\frac{\langle S_d \rangle_+}{\langle S_s \rangle_+} \right]. \quad (6.7)$$

If we follow these lines, we obtain a twofold solution $\gamma = \gamma_1 \vee \gamma_2$, where we may choose $\gamma_1 \in [0^\circ, 180^\circ]$ and $\gamma_2 = \gamma_1 + 180^\circ$; the theoretical uncertainty would mainly be limited by U -spin-breaking corrections to $a_s = a_d$, apart from tiny corrections to $\cos \delta_s = \cos \delta_d$. If we assume – as is usually done – that γ lies between 0° and 180° , as is implied by the Standard-Model interpretation of ε_K , which measures the “indirect” CP violation in the neutral kaon system, we may immediately exclude the γ_2 solution. However, since ε_K may well be affected by new physics, it is desirable to check whether γ actually falls in the interval $[0^\circ, 180^\circ]$. To this end, we may use (2.49) and the signs of the $\langle S_q \rangle_+$ observables, as we have seen in the examples discussed in Section 5.

Let us now consider a non-factorization-like scenario with sizeable CP-conserving strong phases, so that we may also employ (6.2), as the $\langle S_q \rangle_-$ observables would no longer vanish. If we assume that $\delta_s = \delta_d$, we may calculate $(a_s/a_d)R$ both with the help of the $\langle S_q \rangle_+$ observables through (6.1) and with the help of the $\langle S_q \rangle_-$ observables through (6.2). The intersection of the corresponding curves then fixes γ and $(a_s/a_d)R$. Comparing

⁴Note that these relations do not rely on the neglect of (tiny) exchange topologies.

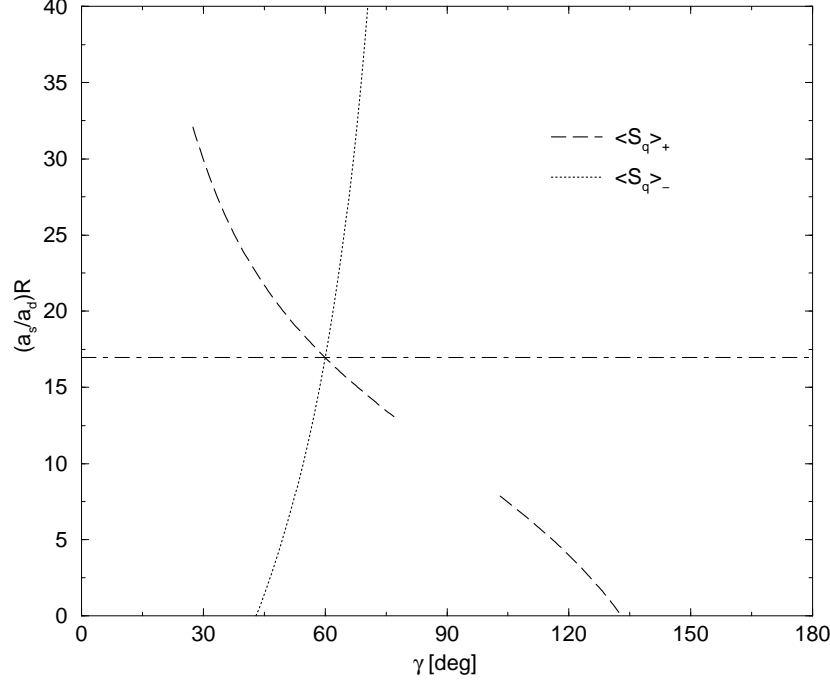


Figure 2: Extraction of γ assuming $\delta_s = \delta_d$ for the non-factorization scenario in Table 1; the dashed and dotted curves were calculated with the help of (6.1) and (6.2), respectively.

the value of $(a_s/a_d)R$ thus extracted with (6.4), we could determine a_s/a_d . If we use the observables given in the lower half of Table 1, which were calculated for $\delta_s = \delta_d = 40^\circ$ and $a_s = a_d = 1$, we obtain the contours shown in Fig. 2, where we have also taken the bounds implied by (5.1) and (5.2) into account, and have represented the curves originating from (6.1) and (6.2) through the dashed and dotted lines, respectively. We observe that the intersection of these contours gives actually our input value of $\gamma = 60^\circ$, without any discrete ambiguity. These observations can easily be put on a more formal level, since (6.1) and (6.2) imply the following *exact* relation:

$$\frac{\tan(\phi_d + \gamma)}{\tan(\phi_s + \gamma)} = \left[\frac{\tan \delta_d}{\tan \delta_s} \right] \left[\frac{\langle S_s \rangle_-}{\langle S_s \rangle_+} \right] \left[\frac{\langle S_d \rangle_+}{\langle S_d \rangle_-} \right] \xrightarrow{U \text{ spin}} \left[\frac{\langle S_s \rangle_-}{\langle S_s \rangle_+} \right] \left[\frac{\langle S_d \rangle_+}{\langle S_d \rangle_-} \right]. \quad (6.8)$$

Consequently, the theoretical uncertainty of the resulting value of γ would *only* be limited by U -spin-breaking corrections to $\tan \delta_s = \tan \delta_d$; in Fig. 2, they would enter through a systematic relative shift of the dashed and dotted contours.

Finally, we may also extract γ *without* assuming that δ_s is equal to δ_d . To this end, we use the *exact* relation

$$\left(\frac{a_s}{a_d} \right) R = \sigma \left| \frac{\sin(2\phi_d + 2\gamma)}{\sin(2\phi_s + 2\gamma)} \right| \sqrt{\frac{\langle S_s \rangle_+^2 \cos^2(\phi_s + \gamma) + \langle S_s \rangle_-^2 \sin^2(\phi_s + \gamma)}{\langle S_d \rangle_+^2 \cos^2(\phi_d + \gamma) + \langle S_d \rangle_-^2 \sin^2(\phi_d + \gamma)}}, \quad (6.9)$$

where we have

$$\sigma = -\text{sgn} \{ \langle S_s \rangle_+ \langle S_d \rangle_+ \sin(\phi_d + \gamma) \sin(\phi_s + \gamma) \} \quad (6.10)$$

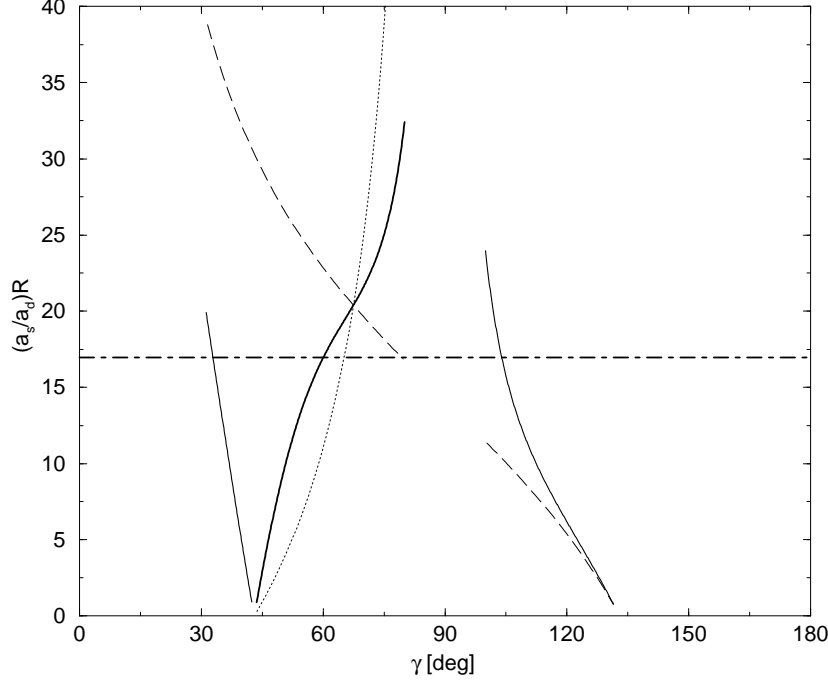


Figure 3: Extraction of γ with the help of (6.9), yielding the solid lines, for an example with $\delta_d = 50^\circ$ and $\delta_s = 30^\circ$, as discussed in the text.

if we assume that $\cos \delta_s$ and $\cos \delta_d$ have the same sign, and

$$\sigma = -\text{sgn} \{ \langle S_s \rangle_- \langle S_d \rangle_- \cos(\phi_d + \gamma) \cos(\phi_s + \gamma) \} \quad (6.11)$$

if we assume that $\sin \delta_s$ and $\sin \delta_d$ have the same sign. Using (6.9), we may calculate $(a_s/a_d)R$ in an *exact* manner as a function of γ from the measured values of the mixing-induced observables $\langle S_s \rangle_\pm$ and $\langle S_d \rangle_\pm$. On the other hand, we have $a_s \approx a_d$ because of the U -spin flavour symmetry, and may efficiently fix R from untagged B_s data samples through (6.4), allowing us to determine γ . Let us illustrate how this strategy works in practice by considering again an example, corresponding to $a_s = a_d = 1$, $\delta_d = 50^\circ$ and $\delta_s = 30^\circ$. Moreover, as in Table 1, we choose $\gamma = 60^\circ$, $\phi_d = 47^\circ$, $\phi_s = 0^\circ$ and $R_b = 0.4$, implying $\langle S_d \rangle_+ = -2.50\%$, $\langle S_d \rangle_- = -0.91\%$, $\langle S_s \rangle_+ = 51.7\%$, $\langle S_s \rangle_- = -17.2\%$. If we apply (5.1) and (5.2) to the B_s observables, we obtain $31^\circ \leq \gamma \leq 80^\circ \vee 100^\circ \leq \gamma \leq 133^\circ$. Constraining γ to this range, the right-hand side of (6.9) yields the solid lines shown in Fig. 3, where we have represented the “measured” value of R through the horizontal dot-dashed line; the three lines emerge if we fix σ through (6.10), yielding the threefold solution $\gamma = 33^\circ \vee 60^\circ \vee 104^\circ$. However, (6.11) leaves only the thicker solid line in the middle, thereby implying the single solution $\gamma = 60^\circ$. In this particular example, the extracted value for γ would be quite stable with respect to variations of $(a_s/a_d)R$, i.e. would not be very sensitive to U -spin-breaking corrections to $a_s = a_d$. We have also included the contours corresponding to (6.1) and (6.2) through the dashed and dotted

curves, as in Fig. 2; their intersection would now give $\gamma = 68^\circ$, deviating by only 8° from the “correct” value. It should be noted that we may also determine the strong phases δ_s and δ_d with the help of

$$\tan \delta_q = - \left[\frac{\langle S_q \rangle_-}{\langle S_q \rangle_+} \right] \tan(\phi_q + \gamma), \quad (6.12)$$

providing valuable insights into non-factorizable U -spin-breaking effects.

In comparison with the conventional $B_q \rightarrow D_q \bar{u}_q$ approaches – apart from issues related to multiple discrete ambiguities – the most important advantage of the strategies proposed above is that they do *not* require the resolution of x_q^2 terms, since the mixing-induced observables $\langle S_d \rangle_\pm$ and $\langle S_s \rangle_\pm$ are proportional to x_d and x_s , respectively. In particular, x_d has *not* to be fixed, and x_s may only enter through $1 + x_s^2$, i.e. a moderate correction, which can straightforwardly be included through untagged B_s rate analyses. Interestingly, the motivation to measure x_s and x_d accurately is here related only to the feature that these parameters would allow us to take into account possible U -spin-breaking corrections to (6.9) through

$$\frac{a_s}{a_d} = \left(\frac{\lambda^2}{1 - \lambda^2} \right) \left| \frac{x_s}{x_d} \right|. \quad (6.13)$$

After all these steps of progressive refinement, we would eventually obtain a theoretically clean value of γ .

For a theoretical discussion of the U -spin-breaking effects affecting the ratio a_s/a_d , we may distinguish – apart from mass factors – between two pieces,

$$\frac{a_s}{a_d} \sim \zeta_1 \times \zeta_2, \quad (6.14)$$

which can be written for the $B_s \rightarrow D_s^{(*)\pm} K^\mp$, $B_d \rightarrow D^{(*)\pm} \pi^\mp$ system – if we apply the factorization approximation – with the help of (2.42), (2.43) and (2.45), (2.46) as follows:

$$\zeta_1^{(*)} \Big|_{\text{fact}} = \frac{f_{\pi^\pm} \xi_d(w_d^{(*)})}{f_{K^\pm} \xi_s(w_s^{(*)})} \quad (6.15)$$

$$\zeta_2 \Big|_{\text{fact}} = \frac{f_{D_s} F_{B_s K^\pm}^{(0)}(M_{D_s}^2)}{f_{D_d} F_{B_d \pi^\pm}^{(0)}(M_{D_d}^2)}, \quad \zeta_2^* \Big|_{\text{fact}} = \frac{f_{D_s^*} F_{B_s K^\pm}^{(1)}(M_{D_s^*}^2)}{f_{D_d^*} F_{B_d \pi^\pm}^{(1)}(M_{D_d^*}^2)}. \quad (6.16)$$

Because of the arguments given in Subsection 2.3, the factorized expression (6.15) for $\zeta_1^{(*)}$ is expected to work well. Studies of the light-quark dependence of the Isgur–Wise function were performed in [33] within heavy-meson chiral perturbation theory, indicating an enhancement of ξ_s/ξ_d at the level of 5%. The application of the same formalism to f_{D_s}/f_{D_d} yields values at the 1.2 level [34], which is of the same order of magnitude as recent lattice calculations (see, for example, [35]). In the case of $\zeta_2^{(*)}$, (6.16) may receive sizeable non-factorizable corrections, since simple colour-transparency arguments are not on solid ground, and the new theoretical developments related to factorization that were

presented in [22] are not applicable. Moreover, we are not aware of quantitative studies of the $SU(3)$ -breaking effects arising from the $B_s \rightarrow K^\pm$, $B_d \rightarrow \pi^\pm$ form factors in (6.16), which could be done, for instance, with the help of lattice or sum-rule techniques. Following the latter approach, sizeable $SU(3)$ -breaking corrections were found for the $B_s \rightarrow K^{*\pm}$, $B_d \rightarrow \rho^\pm$ form factors in [36]. Hopefully, a better theoretical treatment of the U -spin-breaking corrections to a_s/a_d will be available by the time the $B_q \rightarrow D_q \bar{u}_q$ measurements can be performed in practice.

The new strategies proposed above complement other U -spin approaches to extract γ [37, 38], where the U -spin-related $B_s \rightarrow K^+ K^-$, $B_d \rightarrow \pi^+ \pi^-$ system is particularly promising [25, 30, 38]. Since penguin topologies play here a crucial rôle, whereas these topologies do not contribute to the $B_s \rightarrow D_s^{(*)\pm} K^\mp$, $B_d \rightarrow D^{(*)\pm} \pi^\mp$ system, it will be very interesting to see whether inconsistencies for γ will emerge from the data.

7 Conclusions

Let us now summarize the main points of our analysis:

- We have shown that $B_s \rightarrow D_s^\pm K^\mp$, $D_s^{*\pm} K^\mp$, ... and $B_d \rightarrow D^\pm \pi^\mp$, $D^{*\pm} \pi^\mp$, ... decays can be described through the same set of formulae by just making straightforward replacements of variables. We have also pointed out that a factor of $(-1)^L$ arises in the expressions for the mixing-induced observables. In the presence of a non-vanishing angular momentum L of the B_q decay products, this factor has properly to be taken into account in the determination of the sign of $\sin(\phi_q + \gamma)$ from $\langle S_q \rangle_+$.
- Should the width difference $\Delta\Gamma_s$ be sizeable, the combination of the “tagged” mixing-induced observables $\langle S_s \rangle_\pm$ with their “untagged” counterparts $\langle \mathcal{A}_{\Delta\Gamma_s} \rangle_\pm$ offers an elegant determination of $\tan(\phi_s + \gamma)$ in an essentially unambiguous manner, which does not require knowledge of x_s . Another important aspect of untagged rate measurements is the efficient determination of the hadronic parameters x_q . To accomplish this task, we may apply various untagged strategies, which do not rely on a sizeable value of $\Delta\Gamma_q$.
- We have derived bounds on $\phi_q + \gamma$, which can straightforwardly be obtained from the mixing-induced $B_q \rightarrow D_q \bar{u}_q$ observables, and provide essentially the same information as the “conventional” determination of $\phi_q + \gamma$, which suffers from multiple discrete ambiguities. Giving a few examples, we have illustrated the potential power of these constraints, and have seen that stringent bounds on γ may be obtained through a *combined* study of $B_s \rightarrow D_s \bar{u}_s$ and $B_d \rightarrow D_d \bar{u}_d$ modes.
- If we perform a simultaneous analysis of U -spin-related decays, for example of the $B_s \rightarrow D_s^{(*)\pm} K^\mp$, $B_d \rightarrow D^{(*)\pm} \pi^\mp$ system, we may follow various attractive avenues to determine γ from the corresponding mixing-induced observables $\langle S_q \rangle_\pm$. The differences between these methods are due to different implementations of the U -spin relations for the hadronic parameters a_q and δ_q . For example, we may extract

γ by assuming $\tan \delta_s = \tan \delta_d$ or $a_s = a_d$. In comparison with the conventional $B_q \rightarrow D_q \bar{u}_q$ approaches, the most important advantage of these strategies – apart from features related to discrete ambiguities – is that x_d does not have to be fixed, and that x_s may only enter through $1 + x_s^2$, i.e. a moderate correction, which can straightforwardly be included through untagged B_s rate measurements; an accurate determination of x_d and x_s would only be interesting for the inclusion of U -spin-breaking corrections to a_s/a_d . After various steps of refinement, we would eventually arrive at an unambiguous, theoretically clean value of γ , and could also obtain – as a by-product – valuable insights into U -spin-breaking effects.

Since $B_{s,d} \rightarrow D_{s,d} \bar{u}_{s,d}$ modes will be accessible in the era of the LHC, in particular at LHCb, we strongly encourage a simultaneous analysis of B_s and B_d modes – especially of U -spin-related decay pairs – to fully exploit their very interesting physics potential.

References

- [1] M. Kobayashi and T. Maskawa, *Prog. Theor. Phys.* **49** (1973) 652.
- [2] R. Fleischer, *Phys. Rep.* **370** (2002) 537.
- [3] BaBar Collaboration (B. Aubert *et al.*), *Phys. Rev. Lett.* **87** (2001) 091801;
Belle Collaboration (K. Abe *et al.*), *Phys. Rev. Lett.* **87** (2001) 091802.
- [4] Y. Nir, WIS-35-02-DPP [hep-ph/0208080].
- [5] A.J. Buras, TUM-HEP-435-01 [hep-ph/0109197];
A. Ali and D. London, *Eur. Phys. J.* **C18** (2001) 665;
D. Atwood and A. Soni, *Phys. Lett.* **B508** (2001) 17;
M. Ciuchini *et al.*, *JHEP* **0107** (2001) 013;
A. Höcker *et al.*, *Eur. Phys. J.* **C21** (2001) 225.
- [6] R. Fleischer and J. Matias, *Phys. Rev.* **D66** (2002) 054009;
R. Fleischer, G. Isidori and J. Matias, *JHEP* **0305** (2003) 053.
- [7] Ya.I. Azimov, V.L. Rappoport and V.V. Sarantsev, *Z. Phys.* **A356** (1997) 437;
Y. Grossman and H.R. Quinn, *Phys. Rev.* **D56** (1997) 7259;
J. Charles *et al.*, *Phys. Lett.* **B425** (1998) 375;
B. Kayser and D. London, *Phys. Rev.* **D61** (2000) 116012;
H.R. Quinn *et al.*, *Phys. Rev. Lett.* **85** (2000) 5284.
- [8] A.S. Dighe, I. Dunietz and R. Fleischer, *Phys. Lett.* **B433** (1998) 147.
- [9] I. Dunietz, R. Fleischer and U. Nierste, *Phys. Rev.* **D63** (2001) 114015.
- [10] R. Itoh, KEK-PREPRINT-2002-106 [hep-ex/0210025].

- [11] R. Aleksan, I. Dunietz and B. Kayser, *Z. Phys.* **C54** (1992) 653.
- [12] I. Dunietz and R.G. Sachs, *Phys. Rev.* **D37** (1988) 3186 [E: **D39** (1989) 3515];
I. Dunietz, *Phys. Lett.* **B427** (1998) 179;
M. Diehl and G. Hiller, *Phys. Lett.* **B517** (2001) 125;
D.A. Suprun, C.W. Chiang and J.L. Rosner, *Phys. Rev.* **D65** (2002) 054025.
- [13] R. Fleischer and I. Dunietz, *Phys. Lett.* **B387** (1996) 361.
- [14] D. London, N. Sinha and R. Sinha, *Phys. Rev. Lett.* **85** (2000) 1807.
- [15] M. Gronau, D. Pirjol and D. Wyler, *Phys. Rev. Lett.* **90** (2003) 051801.
- [16] R. Fleischer, *Phys. Lett.* **B562** (2003) 234.
- [17] R. Fleischer, *Nucl. Phys.* **B659** (2003) 321.
- [18] A.J. Buras, TUM-HEP-489-02 [hep-ph/0210291].
- [19] L. Wolfenstein, *Phys. Rev. Lett.* **51** (1983) 1945;
A.J. Buras, M.E. Lautenbacher and G. Ostermaier, *Phys. Rev.* **D50** (1994) 3433.
- [20] J.D. Bjorken, *Nucl. Phys. (Proc. Suppl.)* **B11** (1989) 325;
M.J. Dugan and B. Grinstein, *Phys. Lett.* **B255** (1991) 583.
- [21] M. Neubert and B. Stech, *Adv. Ser. Direct. High Energy Phys.* **15** (1998) 294.
- [22] M. Beneke, G. Buchalla, M. Neubert and C.T. Sachrajda, *Nucl. Phys.* **B591** (2000) 313;
C.W. Bauer, D. Pirjol and I.W. Stewart, *Phys. Rev. Lett.* **87** (2001) 201806.
- [23] M. Neubert, *Phys. Rep.* **245** (1994) 259.
- [24] M. Bauer, B. Stech and M. Wirbel, *Z. Phys.* **C34** (1987) 103.
- [25] P. Ball *et al.*, CERN-TH/2000-101 [hep-ph/0003238], in CERN Report on *Standard Model Physics (and more) at the LHC* (CERN, Geneva, 2000), p. 305.
- [26] *The BaBar Physics Book*, eds. P. Harrison and H. Quinn, SLAC report 504 (1998).
- [27] I. Dunietz, *Phys. Rev.* **D52** (1995) 3048.
- [28] M. Beneke and A. Lenz, *J. Phys.* **G27** (2001) 1219.
- [29] Y. Grossman, *Phys. Lett.* **B380** (1996) 99.
- [30] K. Anikeev *et al.*, FERMILAB-Pub-01/197 [hep-ph/0201071].
- [31] BaBar Collaboration (B. Aubert *et al.*), BABAR-PUB-02-010 [hep-ex/0211053];
Belle Collaboration (P. Krokovny *et al.*), *Phys. Rev. Lett.* **89** (2002) 231804.

- [32] BaBar Collaboration (B. Aubert *et al.*), BABAR-CONF-03-015 [hep-ex/0307036].
- [33] E. Jenkins and M.J. Savage, *Phys. Lett.* **B281** (1992) 331.
- [34] B. Grinstein, E. Jenkins, A.V. Manohar, M.J. Savage and M.B. Wise, *Nucl. Phys.* **B380** (1992) 369.
- [35] UKQCD Collaboration (K.C. Bowler *et al.*), *Nucl. Phys.* **B619** (2001) 507.
- [36] P. Ball and V.M. Braun, *Phys. Rev.* **D58** (1998) 094016.
- [37] R. Fleischer, *Eur. Phys. J.* **C10** (1999) 299;
M. Gronau and J.L. Rosner, *Phys. Lett.* **B482** (2000) 71;
P.Z. Skands, *JHEP* **0101** (2001) 008.
- [38] R. Fleischer, *Phys. Lett.* **B459** (1999) 306.